

ISO-CLASS CURVES FOR THE ASSESSMENT OF SEISMIC/ENERGY RETROFITTING OF AN EXISTING MASONRY BUILDING THROUGH A TIMBER FRAME SYSTEM

Linda Giresini^{1,*}, Francesca Corona², Gabriele Guerrini² and Francesco Graziotti²

¹ Department of Structural and Geotechnical Engineering, University of Rome La Sapienza
Via Eudossiana 18, 00184 Rome (Italy)

*Corresponding author, e-mail: linda.giresini@uniroma1.it

² Department of Civil Engineering and Architecture (DICAr), University of Pavia
Via Ferrata 3, 27100 Pavia, Italy (Italy)

e-mail: francesca.corona01@universitadipavia.it, {gabriele.guerrini, francesco.graziotti}@unipv.it

Abstract

Integrated interventions aim at improving both the seismic and the energy performance of existing buildings to optimize costs, environmental impact, and social consequences. This paper introduces the concept of iso-class curves for the selection of optimal integrated interventions, which provide the values of their economic costs and environmental impacts. The method is applied to a civil building located in Central Italy and hit by the 2016 earthquake, during which it exhibited a medium-high damage level with partial collapse. The building presents some critical aspects such as low masonry quality, in-plan irregularity, slender walls, openings close to corners, absence of structural connections and poor structural details. The seismic vulnerability and the energy performance are firstly assessed in the as-built configuration; afterwards, an innovative integrated retrofit consisting in a timber frame with OSB sheathing coupled with insulating panels is considered. The enhancement of seismic and energy performance is expressed through iso-class curves. These curves are easily readable by designers and owners to select the optimum intervention for the desired seismic or energy performance upgrade.

Keywords: iso-class curve; integrated retrofit; environmental impact; sustainable retrofit; upgrade incentives; existing building

1 INTRODUCTION

Recent catastrophic natural events have prompted attention on climate change and related impacts on our society. The influence of the built environment is currently being analyzed by numerous researchers and international organizations, for example the United Nations [1]. According to this recent report, the total energy demand in buildings is about 35% of final demand and the built environment is responsible for 37% of global greenhouses gases (GHG) emissions. Moreover, the global gross floor area has increased from 218 billion square meters in 2015 to 242 billion square meters in 2021. It is therefore evident that the building and construction sector is not on track to achieve decarbonization by 2050, making it an area for immediate action.

Generally, in the current professional practice the structural/seismic retrofit is treated separately from the energy performance improvement of the same building. This may result in non-ecological solutions. Indeed, the mutual influence of energy and seismic performance of existing buildings cannot be disregarded [2]. This situation has pushed many researchers to devise integrated retrofit systems addressing both problems at once. For example, some works aimed at improving reinforced concrete (RC) buildings through independent exoskeletons designed through Life Cycle Thinking (LCT) [3]; some others proposed engineered insulating concrete form panels, installed on the external façade of existing buildings with concrete poured within to constitute a shell exoskeleton [4]. Many other solutions combining seismic and energy retrofit for existing buildings are illustrated in literature reviews [5] [6].

At the same time, numerous methods to design Green Reinforcement of Existing Buildings (GREB) were conceived. For example, Pohoryles et al. [7] proposed a monetary metric for combined assessments based on expected annual losses from energy costs and seismic losses to identify an optimum retrofitting scenario. Caruso et al. [8] conceived a life cycle methodology to find an optimal balance between the reduction of seismic vulnerability and the improvement of energy performance of a building, considering both economic losses and environmental impacts. The latter procedure was recently applied to a RC structure [9] considering several life-cycle stages: initial construction, operation in the pre-retrofit configuration, retrofit application, operation in the post-retrofit configuration, and demolition. The economic loss curves, plotting the total average loss as a function of the annual probability of exceedance of that loss, were estimated by using both the Italian standards and the FEMA P-58 approach (see [8]). The carbon footprint due to construction was instead estimated through the Economic Input-Output (EIO) method for Life Cycle Assessment (LCA), using the US EIO-LCA web-tool [10], [11] to translate sector-specific costs into environmental impacts.

A new trend proposed by Passoni et al. [12] and called “Sustainable Building Renovation”, applicable to any building material, consists in introducing the LCT concept at the beginning of the design procedure, instead of proposing generic retrofitting solutions and calculating economic costs and carbon emissions only at the end. The key concept of this innovative and comprehensive method is the pre-screening of possible retrofitting solutions, allowing for the selection of the most suitable one according to qualitative LCT and holistic principles (such as duration of work, fast assembling, renovation cost, need for occupants’ relocation, waste generation, expected losses due to seismic hazard, etc.).

Another recent approach, specifically conceived for existing masonry structures but easily applicable to other building materials, was proposed in [13] and [14] for masonry walls without openings or windows, then developed in [15] and [16] considering in-plane façade analysis and LCA. In this method, seismic and energy performance indicators combined in iso-cost and iso-performance curves were used as metrics to identify the optimal GREB solutions corresponding to the minimum economic and environmental impacts. The method was further

extended to cover the seismic retrofit of existing masonry structures with poor structural connections (typical of historic buildings), adopting tie-rods and CFRP strips coupled with insulating panels [17]. This extension to the out-of-plane failure of walls relies on a modelling approach that accounts for the effects of their intersection with orthogonal walls [18]–[22] and will be further developed to include dissipative tie-rods [23]–[25].

This paper introduces an advancement of the methodology presented in [15] and in [17]. The procedure to identify the optimal intervention is applied to a whole masonry building, for which iso-class, iso-cost, and iso-performance curves are proposed. More specifically, a structural unit from a terraced house hit by the 2016 Central Italy earthquake is analyzed to show a preliminary application of the method. An integrated intervention is considered, which combines an innovative timber system for seismic upgrade of masonry walls (with or without mortar injections), with insulating panels for energy enhancement (with or without a new heat generator).

2 METHODOLOGY: PRELIMINARY CONSIDERATIONS ON THE USE OF ISO-CLASS CURVES

In [15] the selection of an optimal integrated retrofit is based on iso-cost and iso-performance curves, which relate the environmental and economic impacts to relative seismic and energy performance indicators. More recently, in [17] the use of absolute performance indicators was shown to be more effective and more agile since the demand can be included in them. This paper introduces the iso-class curves as a tool to identify the optimal integrated interventions. Some preliminary aspects are discussed to be furtherly developed in future research by the Authors.

In Italy, existing buildings can be assigned to seismic [26] and energy performance [27] classes, the latter part of the Energy Performance Building Directives at the European level. The energy performance classes go from the most (A4) to the least efficient (G), depending on a global energy performance index and on a non-renewable global energy performance index for the building. Similarly, the seismic class ranges from the highest (A+) to the lowest (G), depending on the ratio between the peak ground acceleration (PGA) capacity and the associated demand for given limit states, and on the expected annual losses.

A structural retrofit aims at increasing the seismic class, while an energy upgrade brings the building to a higher energy performance class. Consequently, any integrated intervention can be associated with a variation of both classes. Since the variation of seismic and/or energy class implies a specific tax reduction/incentive, the building owner or the decision-maker needs a direct insight into the benefit given by a specific integrated intervention.

The iso-class curves plot either the environmental impact or the economic cost associated with the integrated intervention (from 1 to 5 in Figure 1) and with the corresponding variation of n classes (starting from the as-built class). Therefore, as explained in detail in Section 5, the economic cost and the environmental impact of an integrated retrofit can be calculated by considering the class improvement. Obviously, one has higher classes (A or B for instance) when the integrated retrofit improves at a larger extent both the seismic and the energy performance of the existing building.

Life cycle stages can also be included in the calculation considering the most important ones: (i) installation of the integrated retrofit; (ii) use of the building during the reference life of the integrated intervention and (iii) final disposal of the integrated intervention. By distinguishing the impacts associated with the different life cycle stages, one can compare the impacts accounting for the sole installation of the retrofit or for the entire life cycle, which can result in unexpected outcomes [15]. This paper describes in detail the procedure for assessing

the economic and environmental impact of a specific integrated intervention, including its life cycle cost analysis and LCA. The choice of maintenance schedule, the adoption of a reference life of the integrated retrofit with respect to that of the building, and the occurrence of unexpected events during the reference life of the integrated retrofit need to be thoroughly investigated and will be object of future research.

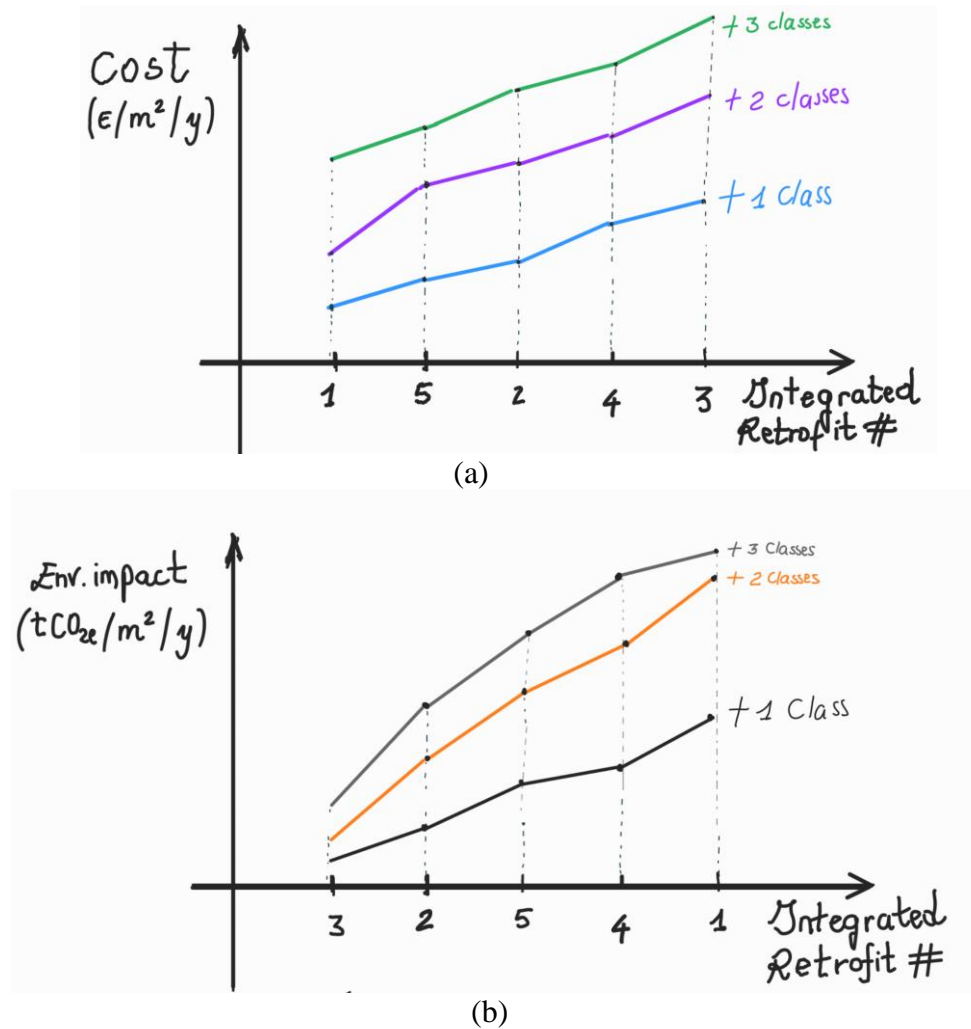


Figure 1: Iso-class curves in terms of (a) economic impact and (b) environmental impact.

3 CASE STUDY: SEISMIC ANALYSIS

This section presents the case-study building selected to assess the environmental and economic impacts of an integrated retrofit, starting from its assessment in the as-built scenario. The global and local seismic analyses are carried out to calculate the seismic class of the existing building. The same building has already been studied in [30] and [31]. Slightly different assumptions have been made in this study mainly concerning the soil type, the stiffness of the floor diaphragms, and the local mechanism analysis method.

3.1 Description of the building

The case study is a two-story structural unit extracted from a masonry terraced house including six units, built in the mid-1960s (Figure 2). The single structural unit has plan dimensions of 7.6 m x 6.9 m and story height of about 3.10 m. The units are not perfectly aligned,

with a shift of about 1.5 m. Differently from [30], the soil class of the building site has been assumed as B and the topographic class as T1 according to [29]. The reference ground acceleration a_g on rock for the ultimate limit state (SLV) is 2.19 m/s^2 . Given a soil factor $S_S = 1.38$ and topographic factor $S_T = 1.0$, the PGA for soil class B is 3.01 m/s^2 .



Figure 2: Case-study masonry terraced house: (a) North-East façade; (b) plan views and orientation.

The North-East and the South-West façades are built with irregular stone masonry and are 45 cm thick (North view and South view respectively in Figure 3), whilst the North-West and the South-East ones are divided in two portions, one in irregular stone masonry (thickness 45 cm) and the second one in hollow clay blocks (thickness 26 cm). Floors consists of precast hollow-clay-block joists with longitudinal steel reinforcement, placed side by side with thin concrete ribs in between and unreinforced concrete topping. More details on the structural components can be found in [30] and [31].

The masonry building was severely damaged during the 2016 Central Italy earthquake, exhibiting relevant in-plane and out-of-plane damage, as visible in Figure 4. Diagonal cracking in piers at the end units, local crumbling of masonry, shear cracking in non-structural partitions and out-of-plane (OOP) overturning of two end façades were detected after the October 2016 earthquake, whose epicenter was at about 20 km from the building.

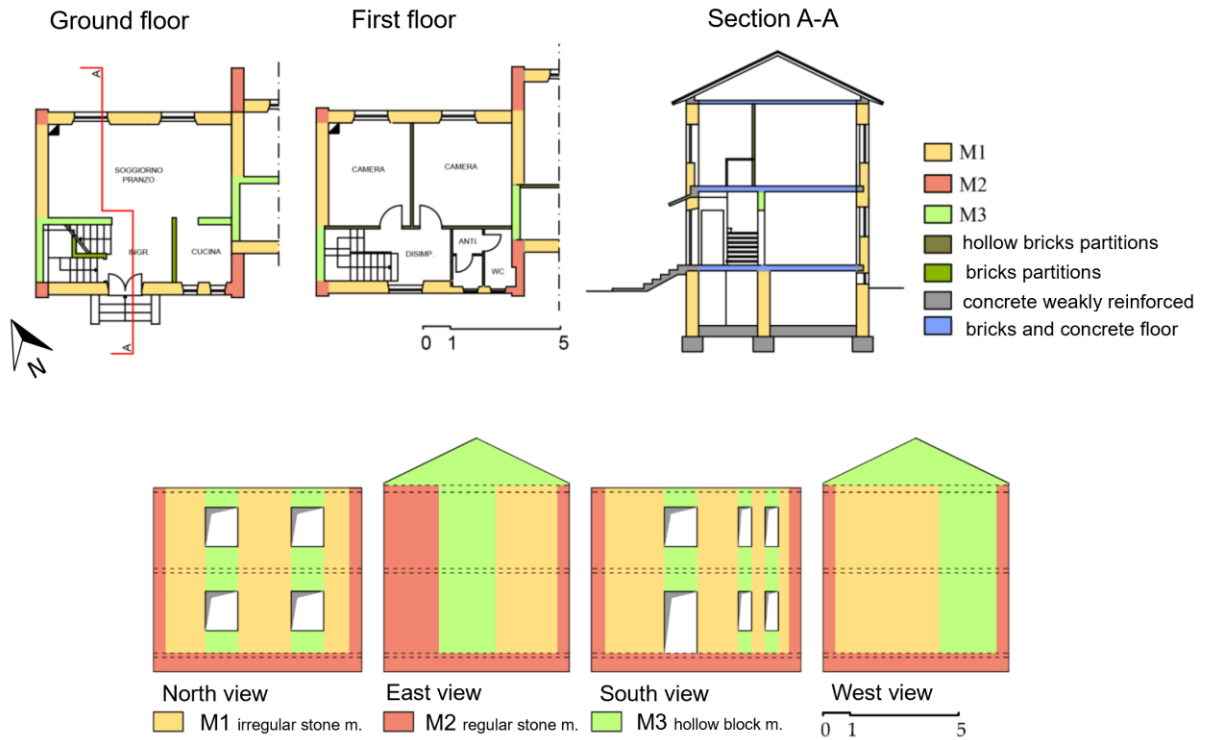


Figure 3: Selected structural unit with material distribution (figure adapted from [31]).

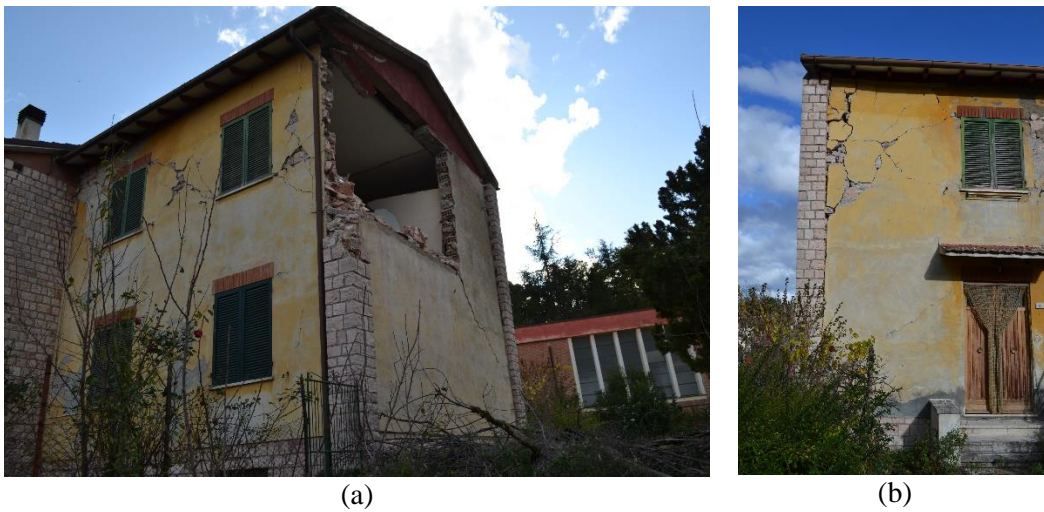


Figure 4: Main failure modes surveyed after the 2016 earthquake: (a) second-story OOP overturning of an end façade; (b) in-plane shear failure and onset of OOP overturning of the North-West façade [31].

3.2 Global seismic analysis

An equivalent-frame model of a single structural unit has been developed in the software 3MURI [32] (Figure 5a, b), consisting of deformable piers and spandrels connected by rigid nodes. Gravity and seismic loads have been applied only at the nodes. Piers and spandrels have been modeled as nonlinear beam elements with lumped inelasticity and bilinear elastic-perfectly plastic behavior. Floor diaphragms have been assigned a slightly higher stiffness than in [31].

The evolution of stiffness, strength and ultimate displacement capacity has been represented through appropriate strength criteria in flexure and shear (dependent on the applied axial load at the current analysis step) and corresponding drift limits. The non-linear static analysis has been performed considering two load patterns, uniform and proportional to the static forces. The X direction has been oriented parallel to the façades with openings (Figure 2b and Figure 5a).

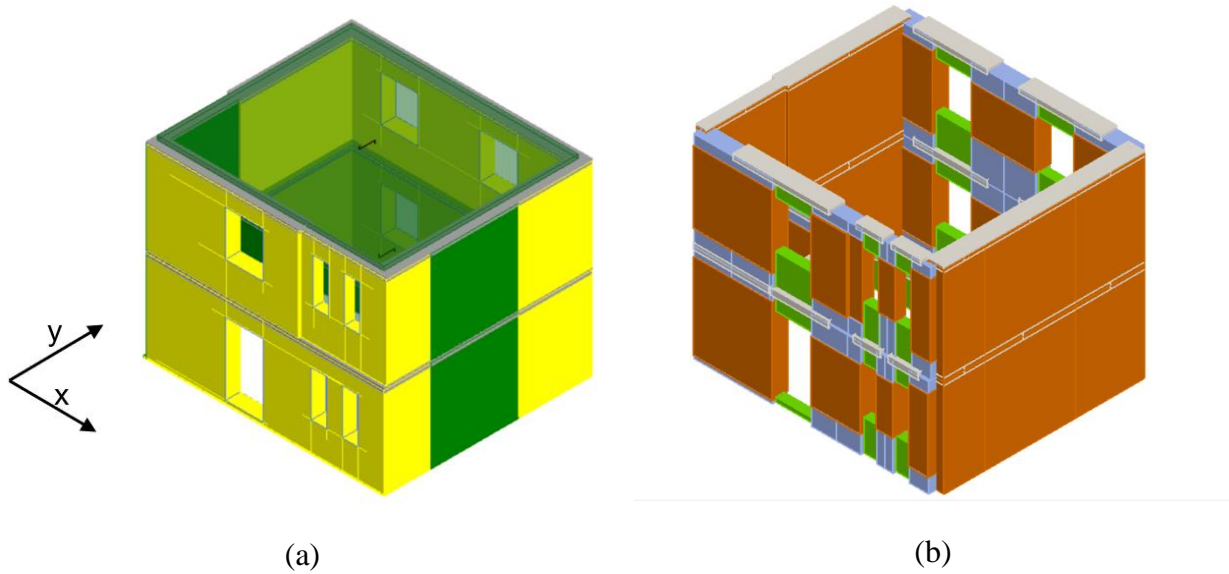


Figure 5: (a) Numerical model of the building in Pieve Torina (Central Italy); (b) subdivision of vertical walls and spandrels in software 3MURI [32].

The most severe pushover analyses in the two directions are the following:

1. For the X direction, the one in the positive verse with horizontal loads proportional to the static forces with eccentricity $e = 31$ cm. The PGA capacities for damage limitation (DL) and severe damage (SD) limit states are $PGA_{C,DL} = 0.7$ m/s² and $PGA_{C,SD} = 1.3$ m/s² respectively.
2. For the Y direction, the one in the positive verse with horizontal loads proportional to the static forces with eccentricity $e = 36$ cm. The PGA capacities for the two limit states in this case are $PGA_{C,DL} = 0.8$ m/s² and $PGA_{C,SD} = 2.2$ m/s² respectively.

Comparing the PGA demands for the two limit states from the design response spectra with the lower capacities obtained in the X direction, one would get a global seismic class C [26], not taking into account the local mechanisms.

3.3 Local mechanism analysis

Differently from [30], a linear kinematic analysis has been performed for the most severe out-of-plane local mechanism found in the building, identified as the simple overturning of the North-West façade, which actually collapsed during the 2016 Central Italy earthquake. The choice of a simple overturning mechanism is supported by the fact that, although there are concrete ring beams at the top of the walls, they are not reinforced and do not guarantee sufficient restraint to induce a vertical bending mechanism; moreover, the upper ring beam broke and collapsed with the wall (Figure 6a, b).

The out-of-plane response has been analyzed considering the four rigid-block mechanisms displayed in Figure 7. The underlying assumptions are: no tensile strength, monolithic mac-

robblocks and negligible friction between walls and horizontal diaphragms. The horizontal hinge has been assumed either at the foundation level (Figure 7a, b) or at the first-floor height (Figure 7c, d). In the latter case, the seismic demand has been calculated through the floor spectra formulation of [28].



Figure 6: Details of the overturning mechanism of the North-West façade: (a) general view and vertically hollow block masonry; (b) concrete beam failure.

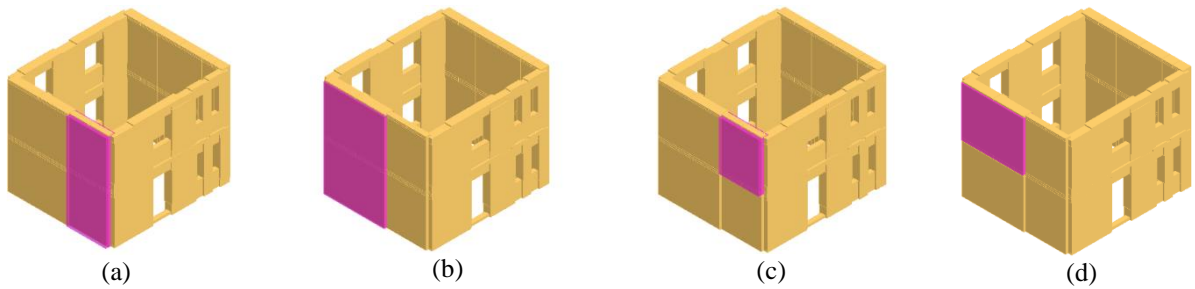


Figure 7: Local mechanisms considered in the linear kinematic analysis of the North-West façade: first and second floor of (a) hollow block and (b) irregular stone wall portion; second floor of (c) hollow block and (d) irregular stone wall portion.

Referring to the mechanism in Figure 7b (full-height mechanism, irregular stone masonry) the spectral acceleration capacity is calculated as $a_0^* = 0.26 \text{ m/s}^2$ [28]. Equating this value to the PGA and iterating on the site spectrum return period, allows determining the PGA capacity for the DL limit state ($PGA_{C,DL} = 0.18 \text{ m/s}^2$). For the SD limit state, the PGA capacity is taken twice as large as the previous value [28], i.e., $PGA_{C,SD} = 0.35 \text{ m/s}^2$.

For the mechanism in Figure 7c (second story mechanism, hollow block masonry) the spectral acceleration capacity is again calculated as $a_0^* = 0.61 \text{ m/s}^2$ [28]. However, now this value must be equated to the peak floor acceleration $a_z(z)$, evaluated at height z above the foundation through the floor response spectrum formulation. Iterating on the site spectrum return period and applying the peak floor acceleration equations [28], allows determining the PGA capacity for the DL limit state ($PGA_{C,DL} = 0.34 \text{ m/s}^2$) and for the SD one ($PGA_{C,SD} = 0.68 \text{ m/s}^2$). The results for all four mechanisms are synthetically reported in Table 1.

The seismic class is defined based on the two parameters IS-V and PAM according to [26] and, for the worse local mechanism is G, whilst in terms of global response was found equal to C. This means that, overall, the building must be assigned to seismic class G.

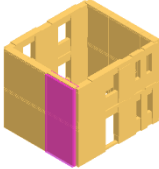
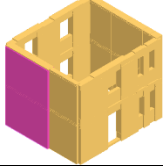
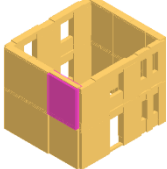
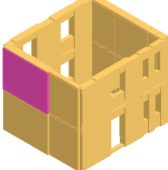
Mechanism	Material	a_0^* m/s ²	$PGA_{C,DL}$ m/s ²	$PGA_{C,SD}$ m/s ²
	hollow block masonry	0.30	0.23	0.47
	irregular stone masonry	0.26	0.18	0.35
	hollow block masonry	0.61	0.34	0.68
	irregular stone masonry	0.53	0.27	0.55

Table 1: Acceleration parameters for OOP local mechanisms.

4 CASE STUDY: ENERGY PERFORMANCE ANALYSIS

This Section presents the energy performance analysis of the existing building in the as-built scenario (without integrated retrofit) with the purpose of obtaining its energy performance class. The classification (from A4, most efficient, to G, the least efficient [33]) is based on the global energy performance index and on the non-renewable global energy performance index of the building.

4.1 Model

The building has been modelled through the software TERMUS-BIM [34] to determine its energy class. The day degrees of the building site are 2189 and the climatic zone is E. The global stratigraphic properties for the as-built configuration are reported in Table 2.

All the openings have been also considered, obtaining values of thermal transmittance of windows included between 2.92 W/m²K and 3.15 W/m²K. Finally, a thermal power station has been assumed for building and water heating. A methane condensing generator has been considered by assuming that the heater has been substituted at least once during the building life. A heat pump for cooling has been also included in the analysis.

Structural element	Thermal transmittance W/m ² K	Unitary heat capacity kJ/m ² K	Periodic thermal transmittance W/m ² K
Floor	1.18	57.42	0.22
Floor (roof)	1.40	69.16	0.38
Roof	0.64	78.20	0.68
Irregular stone (t=45 cm)	2.50	78.79	0.30
Hollow block (t=45 cm)	0.90	55.19	0.08
Hollow block (t=26 cm)	1.37	61.36	0.46
Irregular stone (t=30 cm)	2.96	83.04	0.76

Table 2: Transmittance and heat capacity for the building materials.

To calculate the energy class, the global non-renewable energy performance index $EP_{gl,nren,standard}$ (referred to the standard building) is obtained with the following expression:

$$EP_{gl,nren,standard} = EP_C + EP_H + EP_W \quad (1)$$

where EP_C is the energy performance due to cooling (in summer), EP_H that due to heating (in winter) and EP_W that for water heating. In the case under examination (see Table 3):

$$EP_{gl,nren,standard} = 44.52 + 16.37 + 30.70 = 91.59 \text{ kWh/m}^2 \text{ year} \quad (2)$$

The global total energy performance index EP_{gl} (total energy consumed per square meter per year by the building) equals to:

$$EP_{gl} = EP_{il,risc} + EP_{il,acs} + EP_{il,raff} \quad (3)$$

The three terms on the right-hand side are the total heating, the water heating and the cooling energy performance indexes respectively (Table 3). The energetic class is found by dividing the global energy performance index EP_{gl} by $EP_{gl,nren,standard}$:

$$\frac{EP_{gl}}{EP_{gl,nren,standard}} = \frac{390.88}{91.59} = 4.27 \quad (4)$$

Being this ratio greater than 3.5, the corresponding energy class is G [33]. Consequently, the building is not efficient in terms of energy performance.

EP_{gl}	$EP_{il,risc}$	$EP_{il,acs}$	$EP_{il,raff}$	EP_H	EP_C	EP_W
[kWh/m ² year]	[kWh/m ² year]	[kWh/m ² year]	[kWh/m ² year]	[kWh/m ² year]	[kWh/m ² year]	[kWh/m ² year]
390.88	364.09	1.19	25.60	44.52	16.37	30.70

Table 3: Energy performance indexes in the as-built scenario.

5 DESIGN OF A LOW-IMPACT INTEGRATED INTERVENTION

This Section describes how to assess the environmental and the economic impacts of a low-impact integrated retrofit designed to improve the seismic and energy performance of the existing building under examination. Firstly, the innovative integrated intervention is described; secondly, the building is analyzed in the retrofitted scenario from a seismic and energy performance point of view to quantify its effectiveness, and finally the parameters needed for the iso-class curves are calculated.

5.1 Description of the integrated retrofit

The integrated retrofitting consists of an earthquake resistant solution made of timber frame (with or without mortar injections in the masonry), quite innovative for existing masonry buildings, coupled with insulating EPS panels, OSB panels and new generator. Initially, the two techniques are separately described for the sake of clearness.

As for the first one, the retrofit is made of vertical timber posts connected to the masonry walls to enhance their out-of-plane capacity (as proposed and tested in [35]), recently improved in [36] to increase the in-plane capacity of piers guaranteeing a proper connection between masonry and flooring. The frame is completed with top and bottom sill plates that connect masonry to the floor and the foundation. There are four different connection types: C1 (connections between posts and sill plates), C2 (anchorage between sill plates and floor/foundation), C3 (connections between timber frame and masonry wall), and C4 (connections between timber frame components). The vertical posts improve the masonry wall out-of-plane response by acting as strong-backs in bending. The timber frame and OSB panels increase the in-plane capacity of piers by interacting with masonry through C3 connections. The posts and tie-down connections (C1) contribute to the in-plane flexural strength, while the OSB layer and nailing contribute to the in-plane shear strength. The connection enhancement between masonry and floor offered by the retrofit system is critical in improving seismic performance as it promotes a global box-type response, preventing the onset of undesirable local mechanisms that can greatly reduce the building seismic capacity. The system could be applied in one or both sides of the masonry wall, considering architectural limitations and the required level of improvement. Two different strengthening solutions are then adopted:

1. Only timber frame (including OSB panels);
2. Timber frame (including OSB panels) + mortar injections.

The timber frame described in Subsection 5.1 can be modelled explicitly [37] or by means of the assumption of proper coefficients enhancing the masonry mechanical properties. In this paper, the second approach is considered. For its details, the reader is referred to [38], [39]. The floors are considered rigid in all the mechanical models of the retrofitted scenarios as steel bracings are assumed to be installed at the extrados of each floor.

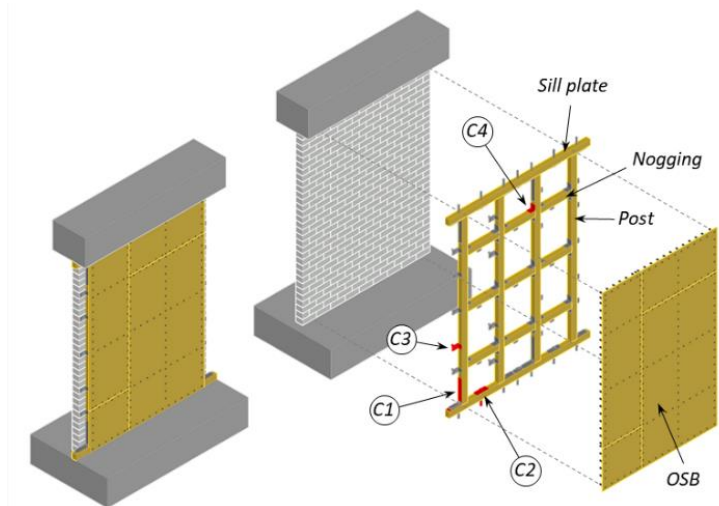


Figure 8: Retrofit components and layout [40].

To improve the energy performance of the building two single retrofits are proposed:

1. Internal insulation with 60 mm-thick polystyrene panels + 20 mm thick OSB panels;
2. Internal insulation with 80 mm-thick polystyrene panels (without seismic retrofit).

For each of them, two further cases are assumed: (i) keeping the old generator or (ii) adding a new generator. In all the scenarios, for the floor at the foundation level, a 100-mm rockwool high density panel is installed to impede the rising damp, and a 40 mm screed above it. For the floor under the roof, a 100-mm polystyrene panel is installed being the floor not habitable.

The individual interventions, that is those only (or mainly, as the timber frame+OSB panels) improving the structural behavior and those only improving the energy efficiency, are combined to become “integrated interventions”. Their influence on the seismic/energy performance of the building is discussed in the following.

5.2 Seismic analysis with integrated retrofits

The seismic class is obtained for each integrated intervention by modifying the numerical model in TREMURI [32] according to the type of strengthening. The outcomes are reported in Table 4. The integrated retrofits are numbered in a progressive order to later compare them in terms of impact. the structural retrofitting types are numbered as reported in Table 4.

As reported in Sections 3.3 and 3.4, the seismic class of the as-built scenario is G by considering the out-of-plane response, whilst it would be C if local failures were prevented. It is easy to observe that independently from the structural intervention, the increase of class-type is high: with the timber frame one passes from class G to B, whereas by adding the mortar injections the class-type becomes A. Although it is not explicated here, the increment nailing in the timber OSB system does not influence the class type in this specific case, differently for the mortar injections. As expected, the addition of energy-efficient interventions (such as EPS and generator) has not any influence on the seismic class.

Individual/integrated retrofit	Class
7 Timber retrofit alone	B
8 Timber retrofit + EPS 6cm + Floors insulation	
9 Timber retrofit + EPS 6cm + Floors insulation + new Generator	
10 Timber retrofit + EPS 4cm + Floors insulation	
11 Timber retrofit + EPS 4cm + Floors insulation + new Generator	
12 Timber retrofit + Floors insulation	
13 Timber retrofit + Floors insulation + new Generator	
7 Timber retrofit + mortar injections (M.inj.)	A
8 Timber retrofit + EPS 6cm + Floors insulation + M.inj.	
9 Timber retrofit + EPS 6cm + Floors insulation + new Generator + M.inj.	
10 Timber retrofit + EPS 4cm + Floors insulation + M.inj.	
11 Timber retrofit + EPS 4cm + Floors insulation + new Generator + M.inj.	
12 Timber retrofit + Floors insulation + M.inj.	
13 Timber retrofit + Floors insulation + new Generator + M.inj.	
1 EPS 6cm + Floors insulation	G
2 EPS 6cm + Floors insulation + new Generator	
3 EPS 4cm + Floors insulation	
4 EPS 4cm + Floors insulation + new Generator	
5 OSB + Floors insulation	
6 OSB + Floors insulation + new Generator	

Table 4: Variation of seismic class considering all the types of integrated retrofit.

5.3 Energy performance analysis with integrated retrofits

The energy class is obtained for each integrated intervention by modifying the model implemented in TERMUS-BIM [34] according to the type of intervention aimed at improving the energy efficiency of the building. The results are listed in Table 5. In this case, the retrofitting types numbered from 8 to 16 (some labels are repeated because the intervention is the same, but the EPS thickness or the generator varies) are associated with more energy classes, from B to E. As a reminder, the energy class in the as-built scenario is G (not to be confused with the G-seismic class). The best improvement is obtained for the highest EPS thickness equal to 6 cm and the new generator, which corresponds to a B-energy class. The intervention with EPS 6 cm and old generator gives the same class as that with EPS 4 cm and new generator (C-energy class). The same result is obtained by comparing the case of EPS 4 cm and old generator with OSB and new generator (D-energy class). The less efficient solutions are, as expected, the mainly structural interventions (OSB and old generator, alone or combined), which correspond to an E-class.

	Individual/integrated retrofit	Class
17	EPS 6cm + Floors insulation + new Generator	B
18	Timber retrofit + EPS 6cm + Floors insulation + new Generator	
19	Timber retrofit + EPS 6cm + Floors insulation + new Generator + M.inj.	
16	EPS 6cm + Floors insulation	C
17	EPS 4cm + Floors insulation + new Generator	
20	Timber retrofit + EPS 6cm + Floors insulation	
21	Timber retrofit + EPS 6cm + Floors insulation + M.inj.	
18	Timber retrofit + EPS 4cm + Floors insulation + new Generator	
19	Timber retrofit + EPS 4cm + Floors insulation + new Generator + M.inj.	
17	OSB + Floors insulation + new Generator	D
16	EPS 4cm + Floors insulation	
18	Timber retrofit + Floors insulation + new Generator	
19	Timber retrofit + Floors insulation + new Generator + M.inj.	
20	Timber retrofit + EPS 4cm + Floors insulation	
21	Timber retrofit + EPS 4cm + Floors insulation + M.inj.	
16	OSB + Floors insulation	E
20	Timber retrofit + Floors insulation	
21	Timber retrofit + Floors insulation + M.inj.	
14	Timber retrofit alone	G
15	Timber retrofit + mortar injections (M.inj.)	

Table 5: Variation of energy class considering all the types of integrated retrofit.

6 ISO-CLASS AND ISO-COST CURVES

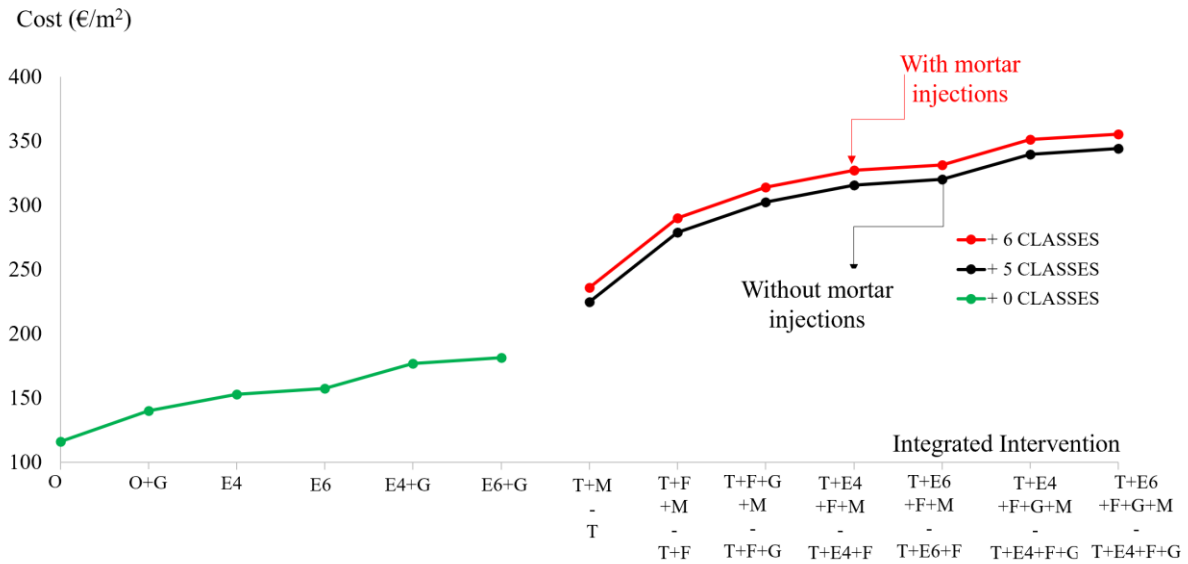
This section summarizes the results obtained in the analysis of the integrated retrofitting to find the optimal interventions by limiting the economic costs and the environmental impacts. Therefore, we make use of iso-class curves which define the change of seismic/energy class for each integrated retrofitting, and we compare them with iso-cost curves in terms of economic costs or environmental impacts.

6.1 Assessment in economic and environmental terms

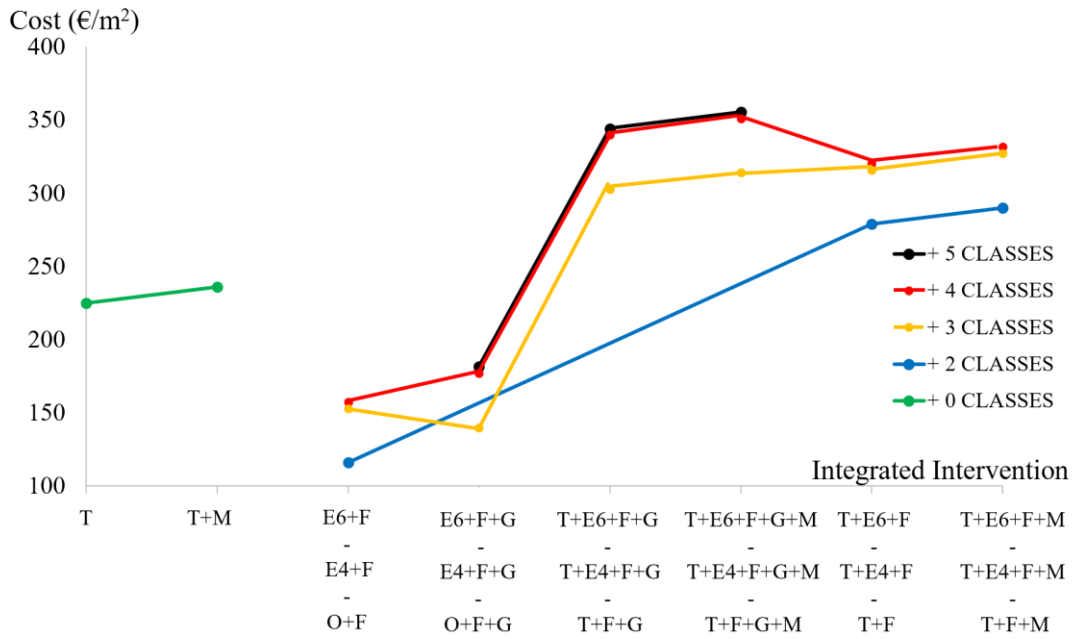
For each integrated retrofit, the corresponding costs were computed per square meter of vertical area of intervention. The unitary costs were taken from 2018 regional price lists [41]. The seismic/energy iso-class curves (Figure 9) report for each integrated intervention the required economic investment (only the initial phase of the life cycle is considered, that is the costs of the raw materials and the installation costs of each integrated retrofit). The green curve represents the economic impact of interventions mainly influencing the energy performance, in fact they do not increase the seismic class. One can notice that there is a variation of cost/m² by less than 5% passing from the corresponding cases with and without mortar injections, so the slight increase in cost can be worthy as a higher class (A-type that is +6 seis-

mic classes with respect to the as-built scenario) is attained with a small additional expense. Looking at Figure 9a, one understands that the best solution is the timber frame + mortar injections, since the economic cost is the minimum and the increase of seismic class is maximum. Nevertheless, this consideration is only partially correct as the seismic iso-class curve must be compared with the energy iso-class curve to find out the best solution also from the point of view of energy performance. Looking at Figure 9b, the best solution in terms of energy performance is the combination of 6 cm-thick EPS panel, new generator and floor insulation, since the economic cost is the minimum and the increase of energy class is maximum.

Figure 10 reports the iso-class curves (seismic class-Figure 10a and energy class-Figure 10b) in terms of environmental impacts or amount of $\text{kgCO}_2\text{eq/m}^2$ (the data are obtained from the database [42]). As for the calculation of the environmental impacts, neither energy saving nor seismic saving are included in this example, as the unique life cycle phase is the installation/implementation of the integrated intervention. The environmental curves provide direct information about the least environmentally impacting solutions, which are again the timber frame+mortar injections for the seismic performance (about $48 \text{ kgCO}_2\text{eq/m}^2$) and 6 cm-thick EPS panel, new generator and floor insulation (about $52 \text{ kgCO}_2\text{eq/m}^2$). The worst retrofit from an environmental point of view is timber retrofit + mortar injections + 6 cm thick EPS panel + floors insulation, because the environmental impact and the economic costs are among the highest ones with the minimum increase of seismic/energy class. The iso-class curves have the advantage of rapidly reading the class variation and the corresponding costs for each integrated retrofit, but they do not provide information about the *integrated benefit* obtained by a specific solution, which can be read from iso-cost (that can also be called “iso-impact” to include both the economic and the environmental impacts) curves, object of future research.

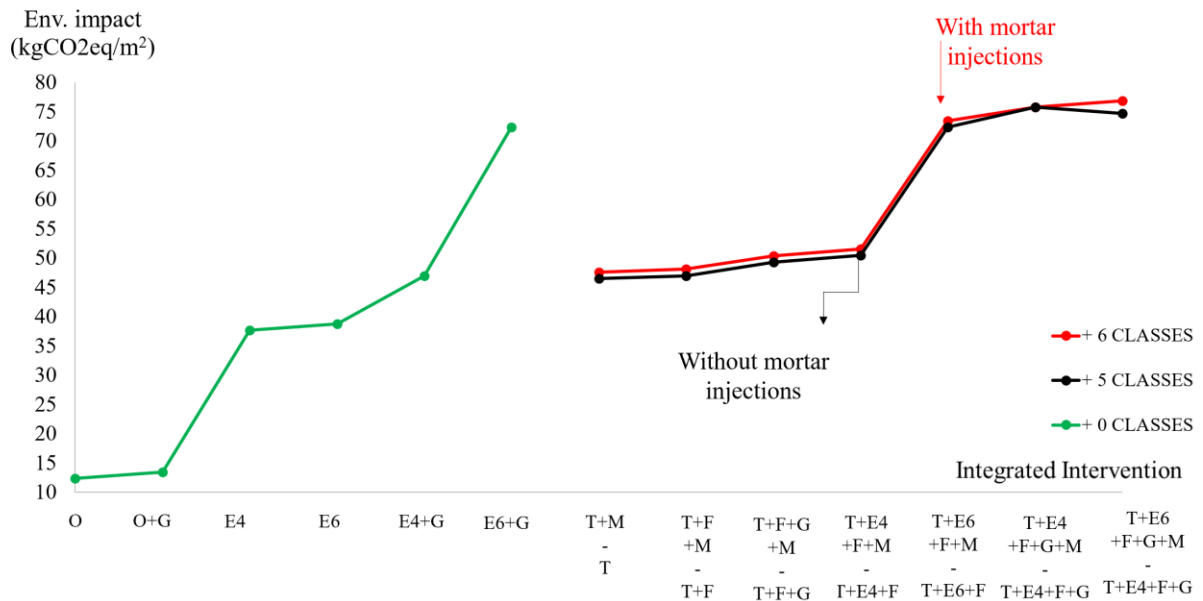


(a)



(b)

Figure 9: Iso-class curves (a) seismic class; (b) energy performance class with economic costs per square meter of vertical area.



(a)

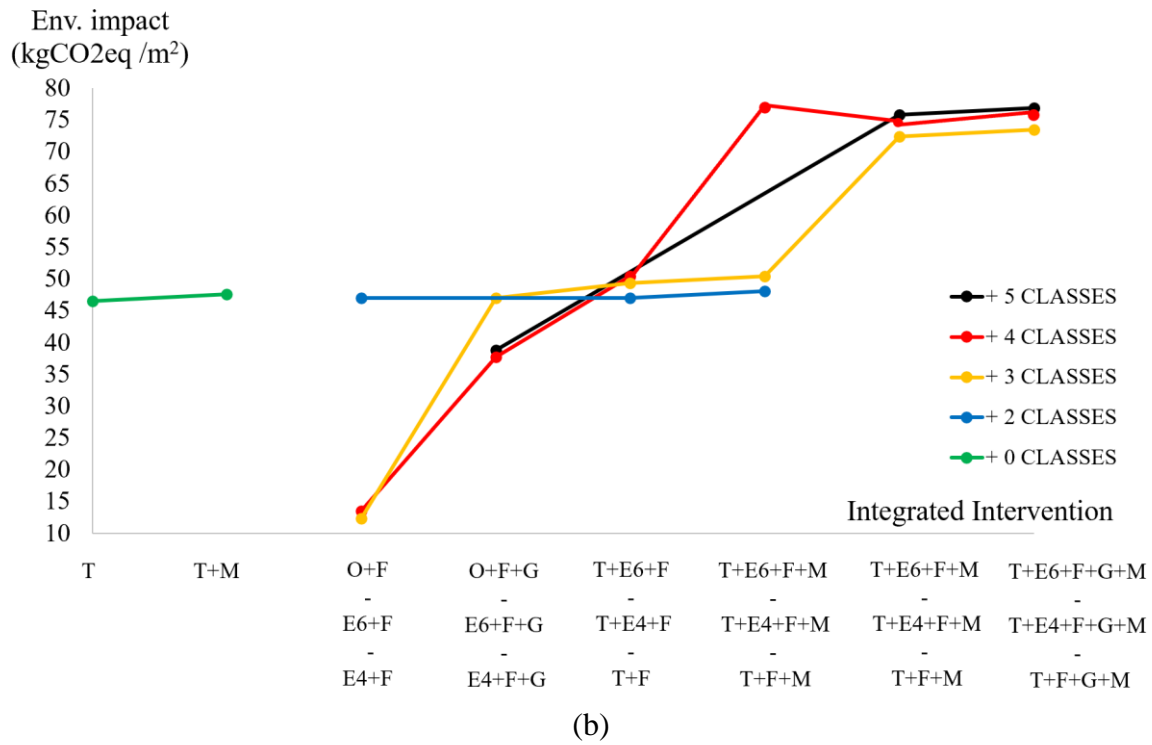


Figure 10: Iso-class curves (a) seismic class; (b) energy performance class with environmental impact per square meter of vertical area.

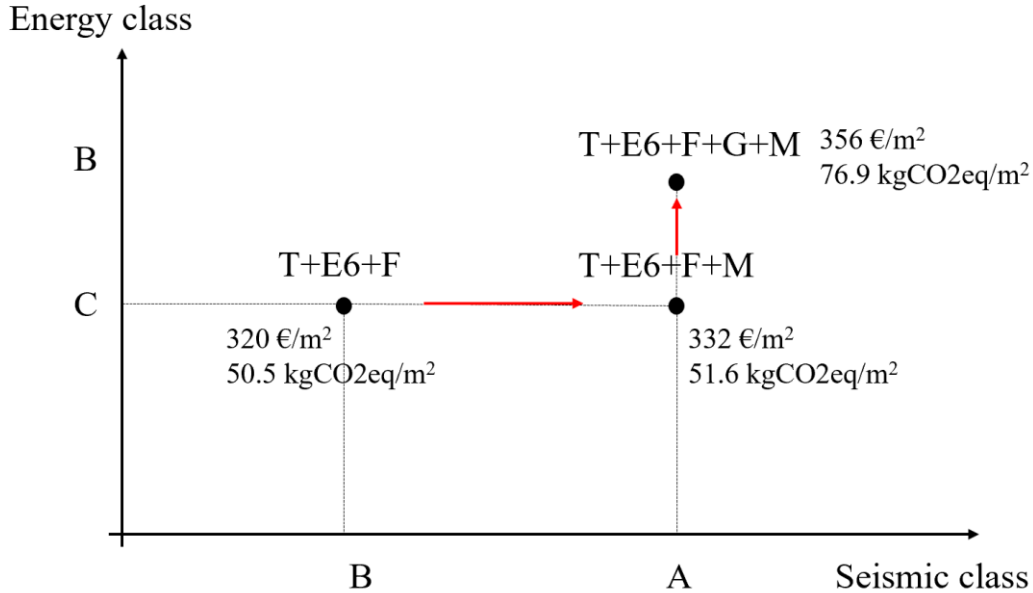


Figure 11: Procedure to identify the optimal integrated intervention.

A practical example to find the optimal intervention is to first fix a minimum seismic class to reach with a retrofit (say B). A specific retrofit (for example timber frame + 6 cm thick EPS panels by keeping the old generator, acronym T+E6+F in Figure 11) has an impact in economic and environmental terms. The need can be (i) to improve only the seismic class or (ii) to improve both seismic and energy class. In the first case, a one-class increment (seismic

class) is obtained by adding mortar injections (M) with a corresponding – not remarkable – increase in environmental impact and economic costs per square meter. In case (ii), the required retrofit consists in adding to the previous one the new generator: the additional expense is low (about 20 €/m²), whilst the extra carbon dioxide emission is about +50% more. However, it is worthy to notice that this result is valid only considering retrofit implementation and neglecting the other life cycles, which could imply an opposite result. Further research will be performed to refine the design methodology of integrated interventions including all the life cycle stages.

CONCLUSIONS

This paper proposed the use of iso-class curves as practical tool to find optimal integrated retrofit for improving the seismic and energy performance of existing buildings. The seismic and energy classes of the strengthened building are determined by numerical and thermal simulations by considering proper integrated retrofits. Afterwards, the economic and environmental costs are computed considering national price lists and databases of CO₂ emissions. A practical example of the procedure is shown by considering a civil building located in Central Italy and hit by the 2016 earthquake, during which it exhibited a medium-high damage level. An innovative timber frame system, coupled with mortar injections, OSB panels, insulating panels and new generator, is considered as main integrated intervention, whose environmental impact and economic cost per square meter is determined and discussed to define a simplified procedure for its optimization.

ACKNOWLEDGEMENTS

The Authors thank the Consortium RELUIS (Rete dei Laboratori Universitari di Ingegneria Sismica e Strutturale) and the Italian Department of Civil Protection, for funding this research in the project: ReLUIS-DPC 2022/2024 -WP5 “Rapid, low-impact and integrated retrofit interventions”.

REFERENCES

- [1] United Nations Environment Programme, “2022 Global Status Report for Buildings and Construction. Global Alliance for Buildings and Construction (Global ABC).”, Dec. 2022. <https://globalabc.org/our-work/tracking-progress-global-status-report> (accessed Dec. 27, 2022).
- [2] A. Belleri and A. Marini, “Does seismic risk affect the environmental impact of existing buildings?,” *Energy Build*, vol. 110, pp. 149–158, Jan. 2016, doi: 10.1016/j.enbuild.2015.10.048.
- [3] A. Marini *et al.*, “Combining seismic retrofit with energy refurbishment for the sustainable renovation of RC buildings: a proof of concept,” *European Journal of Environmental and Civil Engineering*, vol. 26, no. 7, pp. 2475–2495, 2022, doi: 10.1080/19648189.2017.1363665.
- [4] V. Pertile, A. Stella, L. de Stefani, and R. Scotta, “Seismic and Energy Integrated Retrofitting of Existing Buildings with an Innovative ICF-Based System: Design Principles and Case Studies,” *Sustainability*, vol. 13, no. 16, p. 9363, Aug. 2021, doi: 10.3390/su13169363.
- [5] C. Menna *et al.*, “Review of methods for the combined assessment of seismic resilience and energy efficiency towards sustainable retrofitting of existing European buildings,” *Sustainable Cities and Society*, vol. 77. Elsevier Ltd, p. 103556, Feb. 01, 2022. doi: 10.1016/j.scs.2021.103556.

- [6] D. A. Pohoryles, D. A. Bournas, F. da Porto, A. Caprino, G. Santarsiero, and T. Triantafillou, “Integrated seismic and energy retrofitting of existing buildings: A state-of-the-art review,” *Journal of Building Engineering*, vol. 61. Elsevier Ltd, p. 105274, Dec. 01, 2022. doi: 10.1016/j.jobee.2022.105274.
- [7] D. A. Pohoryles, C. Maduta, D. A. Bournas, and L. A. Kouris, “Energy performance of existing residential buildings in Europe: A novel approach combining energy with seismic retrofitting,” *Energy Build*, vol. 223, p. 110024, Sep. 2020, doi: 10.1016/j.enbuild.2020.110024.
- [8] M. Caruso, R. Pinho, F. Bianchi, F. Cavalieri, and M. T. Lemmo, “A Life Cycle Framework for the Identification of Optimal Building Renovation Strategies Considering Economic and Environmental Impacts,” *Sustainability*, vol. 12, no. 23, p. 10221, Dec. 2020, doi: 10.3390/su122310221.
- [9] M. Caruso, R. Pinho, F. Bianchi, F. Cavalieri, and M. T. Lemmo, “Integrated economic and environmental building classification and optimal seismic vulnerability/energy efficiency retrofitting,” *Bulletin of Earthquake Engineering*, vol. 19, no. 9, pp. 3627–3670, Jul. 2021, doi: 10.1007/s10518-021-01101-4.
- [10] Carnegie Mellon University Green Design Institute (CMUGDI), “Free Economic Input-Output Life Cycle Assessment,” 2008. <http://www.eiolca.net/> (accessed Dec. 27, 2022).
- [11] C. Weber, D. Matthews, A. Venkatesh, C. Costello, and H. Matthews, “The 2002 US benchmark version of the economic input-output life cycle assessment (EIO-LCA) model. Green Design Institute at Carnegie Mellon University.” <http://www.eiolca.net/docs/index.html> (accessed Dec. 27, 2022).
- [12] C. Passoni, A. Marini, A. Belleri, and C. Menna, “Redefining the concept of sustainable renovation of buildings: State of the art and an LCT-based design framework,” *Sustain Cities Soc*, vol. 64, p. 102519, Jan. 2021, doi: 10.1016/j.scs.2020.102519.
- [13] F. Mistretta, F. Stochino, and M. Sassu, “Structural and thermal retrofitting of masonry walls: An integrated cost-analysis approach for the Italian context,” *Build Environ*, vol. 155, pp. 127–136, May 2019, doi: 10.1016/j.buildenv.2019.03.033.
- [14] M. Sassu, F. Stochino, and F. Mistretta, “Assessment Method for Combined Structural and Energy Retrofitting in Masonry Buildings,” *Buildings*, vol. 7, no. 3, p. 71, Aug. 2017, doi: 10.3390/buildings7030071.
- [15] L. Giresini, F. Stochino, and M. Sassu, “Economic vs environmental isocost and isoperformance curves for the seismic and energy improvement of buildings considering Life Cycle Assessment,” *Eng Struct*, vol. 233, p. 111923, Apr. 2021, doi: 10.1016/j.engstruct.2021.111923.
- [16] L. Giresini, S. Paone, and M. Sassu, “Integrated cost-analysis approach for seismic and thermal improvement of masonry building Façades,” *Buildings*, vol. 10, no. 8, p. 143, Aug. 2020, doi: 10.3390/BUILDINGS10080143.
- [17] L. Giresini, C. Casapulla, and P. Croce, “Environmental and Economic Impact of Retrofitting Techniques to Prevent Out-of-Plane Failure Modes of Unreinforced Masonry Buildings,” *Sustainability*, vol. 13, no. 20, p. 11383, Oct. 2021, doi: 10.3390/su132011383.
- [18] C. Casapulla, L. U. Argiento, A. Maione, and E. Speranza, “Upgraded formulations for the onset of local mechanisms in multi-storey masonry buildings using limit analysis,” *Structures*, vol. 31, pp. 380–394, Jun. 2021, doi: 10.1016/j.istruc.2020.11.083.
- [19] C. Casapulla, A. Maione, L. U. Argiento, and E. Speranza, “Corner failure in masonry buildings: An updated macro-modeling approach with frictional resistances,” *European Journal of Mechanics, A/Solids*, vol. 70, pp. 213–225, 2018, doi: 10.1016/j.euromechsol.2018.03.003.

- [20] C. Casapulla and L. U. Argiento, “The comparative role of friction in local out-of-plane mechanisms of masonry buildings. Pushover analysis and experimental investigation,” *Eng Struct*, vol. 126, pp. 158–173, 2016, doi: 10.1016/j.engstruct.2016.07.036.
- [21] C. Casapulla, “Local out-of-plane failure modes in traditional block-masonry buildings,” in *Masonry Construction in Active Seismic Regions; Woodhead Publishing Series in Civil and Structural Engineering*, R. Rupakhety and D. Gautam, Eds. Elsevier, 2021, pp. 289–322.
- [22] C. Casapulla, A. Maione, and L. U. Argiento, “Performance-based Seismic Analysis of Rocking Masonry Façades Using Non-linear Kinematics with Frictional Resistances: A Case Study,” *International Journal of Architectural Heritage*, vol. 15, no. 9, pp. 1349–1363, 2021, doi: 10.1080/15583058.2019.1674944.
- [23] L. Giresini, “Effect of dampers on the seismic performance of masonry walls assessed through fragility and demand hazard curves,” *Eng Struct*, vol. 261, p. 114295, Jun. 2022, doi: 10.1016/j.engstruct.2022.114295.
- [24] L. Giresini, F. Solarino, F. Taddei, and G. Mueller, “Experimental estimation of energy dissipation in rocking masonry walls restrained by an innovative seismic dissipator (LICORD),” *Bulletin of Earthquake Engineering*, vol. 19, no. 5, pp. 2265–2289, Mar. 2021, doi: 10.1007/s10518-021-01056-6.
- [25] L. Giresini, F. Taddei, F. Solarino, G. Mueller, and P. Croce, “Influence of Stiffness and Damping Parameters of Passive Seismic Control Devices in One-Sided Rocking of Masonry Walls,” *Journal of Structural Engineering*, vol. 148, no. 2, p. 04021257, Feb. 2022, doi: 10.1061/(asce)st.1943-541x.0003186.
- [26] E. Cosenza *et al.*, “The Italian guidelines for seismic risk classification of constructions: technical principles and validation,” *Bulletin of Earthquake Engineering*, vol. 16, no. 12, pp. 5905–5935, Dec. 2018, doi: 10.1007/s10518-018-0431-8.
- [27] “Direttiva (UE) 2018/844 del Parlamento Europeo e del Consiglio.”
- [28] General Assembly of the Superior Council of Public, *Circolare attuativa del D.M. 17/01/2018 (NTC 2018)*. 2019.
- [29] DMIT, “Decreto del Ministro delle Infrastrutture e dei Trasporti 17 gennaio 2018. Aggiornamento delle ‘Norme tecniche per le costruzioni’. Gazzetta Ufficiale della Repubblica Italiana, n. 42 del 20 febbraio 2018, Supplemento Ordinario n. 8.” 2018.
- [30] M. R. Valluzzi, L. Sbrogiò, and Y. Saretta, “Intervention Strategies for the Seismic Improvement of Masonry Buildings Based on FME Validation: The Case of a Terraced Building Struck by the 2016 Central Italy Earthquake,” *Buildings*, vol. 11, no. 9, p. 404, Sep. 2021, doi: 10.3390/buildings11090404.
- [31] M. R. Valluzzi, L. Sbrogiò, and Y. Saretta, “Report DPC RELUIS 2019-2021 - WP5: Interventi di rapida esecuzione a basso impatto ed integrati - Caso studio: edilizia residenziale a schiera,” 2021.
- [32] S. Lagomarsino, A. Penna, A. Galasco, and S. Cattari, “TREMURI program: An equivalent frame model for the nonlinear seismic analysis of masonry buildings,” *Eng Struct*, vol. 56, pp. 1787–1799, Nov. 2013, doi: 10.1016/j.engstruct.2013.08.002.
- [33] DI2015, “Decreto interministeriale 26 giugno 2015 - Adeguamento linee guida nazionali per la certificazione energetica degli edifici.”
- [34] ACCAsoftware, “TERMUS-BIM.” 2021.
- [35] D. Y. Dizhur, M. Giaretton, I. Giongo, and J. M. Ingham, “Seismic retrofit of masonry walls using timber strong-backs,” *SESOC Journal*, vol. 30, no. 2, pp. 30–44, 2017, doi: 10.3316/SESOC.2017_V030N02;CTYPE:STRING:JOURNAL.
- [36] M. Miglietta, N. Damiani, G. Guerrini, and F. Graziotti, “Full-scale shake-table tests on two unreinforced masonry cavity-wall buildings: effect of an innovative timber retrofit,” *Bulletin*

- of Earthquake Engineering*, vol. 19, no. 6, pp. 2561–2596, Apr. 2021, doi: 10.1007/s10518-021-01057-5.
- [37] N. Damiani, M. Miglietta, G. Guerrini, and F. Graziotti, “Numerical Assessment of the Seismic Performance of a Timber Retrofit Solution for Unreinforced Masonry Buildings,” *International Journal of Architectural Heritage*, 2022, doi: 10.1080/15583058.2022.2106461.
- [38] N. Damiani, G. Guerrini, and F. Graziotti, “An innovative timber system for the seismic retrofit of URM buildings. Part 1: concept, design, and analytical formulations,” *Submitted to Engineering Structures*, 2023.
- [39] N. Damiani, G. Guerrini, M. Miglietta, and F. Graziotti, “An innovative timber system for the seismic retrofit of URM buildings. Part 2: validation of analytical formulations,” *Submitted to Engineering Structures*, 2023.
- [40] G. Guerrini, N. Damiani, M. Miglietta, and F. Graziotti, “Cyclic response of masonry piers retrofitted with timber frames and boards,” *Proceedings of the Institution of Civil Engineers - Structures and Buildings*, vol. 174, no. 5, pp. 372–388, May 2021, doi: 10.1680/jstbu.19.00134.
- [41] PREZ, “Bulletin of unitary costs in Tuscany (Prezziario Lavori Pubblici Regione Toscana) and Bulletin of unitary costs in Lombardia (Prezziario Lavori Pubblici Regione Lombardia) .” 2020.
- [42] ONECLICK LCA, “Computer Program; One Click LCA Ltd.: Helsinki, Finland.” 2021.